

# IR and EXAFS Spectroscopic Studies of Glyphosate Protonation and Copper(II) Complexes of Glyphosate in Aqueous Solution

Julia Sheals,<sup>\*,†</sup> Per Persson,<sup>†</sup> and Britt Hedman<sup>‡</sup>

Department of Chemistry, Inorganic Chemistry, Umeå University, S-901 87 Umeå, Sweden, and Stanford Synchrotron Radiation Laboratory, SLAC, Stanford University, Stanford, California 94309

Received July 28, 2000

The varying degrees of protonation of *N*-(phosphonomethyl)glycine (PMG, glyphosate) were investigated with infrared (IR) spectroscopy and ab initio frequency calculations. The zwitterionic nature of PMG in solution was confirmed, and intramolecular hydrogen bonding was identified. Successive protonation of the PMG molecule follows the order amine, phosphonate, carboxylate. Intramolecular hydrogen bonding is indicated to exist at all stages of protonation: between both  $\text{RCO}_2^-$  and  $\text{RNH}_2^+$  and  $\text{RPO}_3^{2-}$  and  $\text{RNH}_2^+$  in  $\text{HL}^{2-}$  (where L represents the ligand PMG); between  $\text{RCO}_2^-$  and  $\text{RNH}_2^+$  in  $\text{H}_2\text{L}^-$ ; predominantly between  $\text{RPO}_3^{2-}$  and  $\text{RNH}_2^+$  in  $\text{H}_3\text{L}$ . There are strong indications that the zwitterion is intact throughout the pH range investigated. Results from IR and extended X-ray absorption fine structure (EXAFS) spectroscopies provide new evidence for structures of *N*-(phosphonomethyl)glycine-copper(II) complexes. The structures of 1:1 complexes,  $\text{CuL}^-$  and  $\text{CuHL}$ , are essentially the same, differing only in protonation of the phosphonate group. Copper(II) lies at the center of a Jahn–Teller distorted octahedron with all three donor groups (amine, carboxylate, phosphonate) of PMG chelating with copper(II) to form two five-membered chelate rings oriented in the equatorial plane. EXAFS indicates that oxygen (most likely a water molecule) is a fourth ligand, which would thus occupy the fourth corner in the equatorial plane of the elongated octahedron.  $\text{CuL}_2^{4-}$  most probably forms an isomeric mixture in solution, and there are indications that this mixture is dominated by complexes where two PMG ligands are bound to copper(II) via equatorial and axial positions, with both phosphonate and carboxylate donor groups responsible for chelation at axial positions.

## Introduction

The monitoring and control of pollutants in the aquatic environment is becoming of increasing concern. Detailed investigations of interactions between both naturally occurring and anthropogenic species found in the environment provide information regarding the chemical structure and speciation, and thus the transport, bioavailability, and potential toxicity of pollutants. To fully understand the chemical processes that occur in groundwater, soils, and surface waters, it is important to examine the role of the solid–water interface as well as interactions in the aqueous phase.

The present paper is the first in a series of papers investigating ternary surface complexes formed during the adsorption of copper(II) and an organic ligand, *N*-(phosphonomethyl)glycine (PMG), onto mineral oxide surfaces. As it is beneficial to first study the adsorbates in solution before attempting to determine their behavior at the surface, only the solution chemistry of copper(II) and PMG is described here. PMG, also known as glyphosate, is a component of organophosphorus herbicides widely used in agriculture. PMG is capable of killing weeds by inhibiting the shikimic acid pathway, a biochemical pathway present in plants but not in animals. It is applied to kill crop weeds while the crops themselves are engineered to withstand exposure to the PMG.<sup>1</sup> It is known to be immobilized in soils<sup>2</sup> and inactivated by microorganisms to form nonphytotoxic

products.<sup>3</sup> There are several reports in the literature discussing the potential toxicity of PMG.<sup>4,5</sup>

Figure 1 represents the speciation of PMG, which forms a pH-dependent zwitterion in solution. It should be noted that the PMG molecule possesses three donor groups, an amine group, a carboxylate group, and a phosphonate group, which are responsible for complexation reactions with trace metal ions and mineral oxide surfaces. Some trace metal ions, although essential to life, are harmful at excessive concentrations,<sup>6</sup> and chelating agents such as PMG can potentially be used to reduce the bioavailable concentration of trace metals in aquatic and soil environments. Copper(II) provides an ideal example of a trace metal ion, arising from both natural and anthropogenic sources.

The interactions of copper(II) and PMG, with each other and with mineral oxides, and how these affect the bioavailability of each of these substances are just an example of the numerous interactions occurring in surface and groundwaters. Attempting to fully understand such chemical processes in the environment requires a holistic approach, combining results from both molecular-level and macroscopic investigations. The results of this and similar molecular-level studies allow constraints to be applied in the modeling of thermodynamic data. Such chemical

\* Author to whom correspondence should be addressed.

† Umeå University.

‡ Stanford University.

(1) Greenpeace Report—Not Ready for Round-Up Fact Sheet. Greenpeace, 1997.

(2) Glass R. L. *J. Agric. Food Chem.* **1987**, *35*, 497–500.

(3) Morillo, E.; Undabeytia, T.; Maqueda, C. *Environ. Sci. Technol.* **1997**, *31*, 3588–3592.

(4) Carlisle, S. M.; Trevors, J. T. *Water, Air, Soil Pollut.* **1988**, *39*, 409–420.

(5) Carlisle, S. M.; Trevors, J. T. *Water, Air, Soil Pollut.* **1986**, *29*, 189–203.

(6) O'Neill, P. *Environmental Chemistry*; Chapman & Hall: New York, 1993.

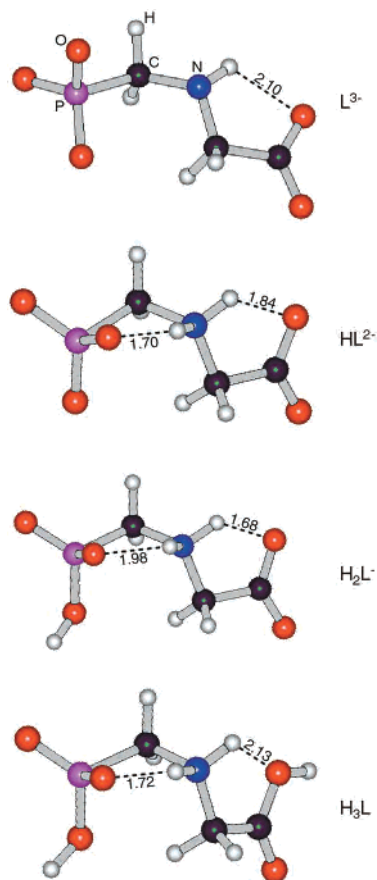


**Figure 1.** Theoretical structures of PMG obtained by the Hartree–Fock theory (basis set 3-21G\*). The bond distances (in angstroms) show the distances between atoms potentially capable of intramolecular hydrogen bonding. The four water molecules included in the calculations have been omitted for the sake of clarity.

models are currently being developed as a tool for determining speciation in natural waters.

Although copper(II)–PMG complexes have been discussed in the literature previously,<sup>7–13</sup> there is an obvious need to provide additional support for proposed structures. The structure of a Cu(II) chelate of PMG as determined by single-crystal X-ray diffraction methods is described by Clarke et al.<sup>7</sup> The presence of two chelate rings involving Cu(II) and the amine, carboxylate, and phosphonate groups was demonstrated. Similarly, in solution, the structure of the negatively charged 1:1 complex, CuL<sup>−</sup> (where L represents a PMG ligand), is suggested to consist of two chelate rings in an equatorial plane where the copper(II) ion is complexed through the amine, the carboxylate, and the phosphonate group while a water molecule occupies a fourth position in this equatorial plane.<sup>8–11</sup> However, these studies did not provide direct structural information such as bond distances and coordination numbers.

There is less agreement regarding the structure of the neutral, protonated 1:1 complex, CuHL. Daniele et al.<sup>8</sup> discuss possible

structures but favor a structure similar to that of CuL<sup>−</sup> with all three donor groups involved. Motekaitis and Martell,<sup>9</sup> on the other hand, state that only the phosphonate oxygens are involved in chelation within the CuHL complex and that the proton resides on the amine group. McBride<sup>10</sup> discusses yet another alternative where the copper(II) ion is coordinated via the amine and either the phosphonate or the carboxylate group to form only one chelate ring. Of these two possibilities, the author considers coordination via carboxylate to be the more probable.

The structure of the 1:2 complex, CuL<sub>2</sub><sup>4−</sup>, is less well understood. Spectrophotometric measurements by Daniele et al.<sup>8</sup> showed no evidence of two nitrogen donors in the equatorial plane. The electron spin resonance studies by McBride,<sup>10</sup> however, indicated the presence of two amine and probably two carboxylate groups in the equatorial plane. Heineke, Franklin, and Raymond's study of the coordination chemistry of glyphosate<sup>14</sup> (primarily focusing on metal(III) complexes) highlighted the likelihood of an isomeric mixture of CuL<sub>2</sub><sup>4−</sup> complexes.

As an attempt to solve some of the discrepancies in the literature and to form a sound basis for continued work involving ternary surface complexes, the current paper presents new evidence concerning the protonation steps of PMG and the structures of copper(II) complexes of PMG, CuHL, CuL<sup>−</sup>, and CuL<sub>2</sub><sup>4−</sup>, in aqueous solution. IR and EXAFS spectroscopies are utilized as complementary techniques whereby IR monitors the behavior of the donor groups of PMG, while EXAFS studies the environment surrounding copper(II). This is the first time EXAFS results are presented for this system and previously undetermined bond distances and coordination numbers are reported. The IR analyses play a crucial role in distinguishing between the varying degrees of protonation, both for PMG alone and for the 1:1 Cu(II)–PMG complexes.

## Experimental Section

**Preparation of Solutions.** Series of PMG and copper–PMG solutions were prepared for examination with IR and EXAFS spectroscopies. For the IR experiments, PMG solutions were prepared both in H<sub>2</sub>O and in D<sub>2</sub>O. Speciation diagrams were generated with the program Solgaswater,<sup>15</sup> using equilibrium constants found in the literature,<sup>16,17</sup> (Table 1a) to determine the pH and mixing ratios that allow each individual complex to dominate in solution, with concentrations of interfering species at a minimum (Figure 2). On the basis of the results of these equilibrium calculations, solutions containing CuHL, CuL<sup>−</sup>, CuL<sub>2</sub><sup>4−</sup>; H<sub>3</sub>L, H<sub>2</sub>L<sup>−</sup>, HL<sup>2−</sup>, L<sup>3−</sup>; D<sub>3</sub>L, D<sub>2</sub>L<sup>−</sup>, DL<sup>2−</sup>, L<sup>3−</sup>, as the dominant species were prepared. The resulting concentrations and pH (or pD) values are listed in Table 1b.

The solutions were prepared at 25 °C from PMG (Sigma) with 95% purity and CuCl<sub>2</sub>·2H<sub>2</sub>O (Aldrich) with >99% purity, and, to the extent possible, with a constant ionic medium of 0.1 M NaCl. A combination glass electrode was used to measure pH. This was externally calibrated by titrating standardized hydrochloric acid in 0.1 M NaCl. For solutions with pH > 7, argon was bubbled through the solutions to avoid carbonates. NaOH was used to adjust samples to the desired pH. Boiled Milli-Q plus 185 water was used in the preparation of all H<sub>2</sub>O-based solutions.

For the D<sub>2</sub>O-based solutions, solid H<sub>3</sub>L was first dissolved in ~3 M NaOH and water was removed by boiling, followed by drying overnight at ~90 °C. The resulting solid was then dissolved in D<sub>2</sub>O (99.9 atom % D; Aldrich), and DCl (diluted from 35% DCl in D<sub>2</sub>O; Aldrich) was added to reach the required pD.

(7) Clarke, E. T.; Rudolf, P. R.; Martell, A. E.; Clearfield, A. *Inorg. Chim. Acta* **1989**, *164*, 59–63.

(8) Daniele, P. G.; De Stefano, C.; Prenesti, E.; Sammartano, S. *Talanta* **1997**, *45*, 425–431.

(9) Motekaitis, R. J.; Martell, A. E. *J. Coord. Chem.* **1985**, *14*, 139–149.

(10) McBride, M. B. *Soil Sci. Soc. Am. J.* **1991**, *55*, 979–985.

(11) Glass, R. L. *J. Agric. Food Chem.* **1984**, *32*, 1249–1253.

(12) Jezowska-Bojczuk, M.; Kiss, T.; Kozłowski, H.; Decock, P.; Barycki, J. *J. Chem. Soc., Dalton Trans.* **1994**, *6*, 811.

(13) Buglyó, P.; Kiss, T.; Dyba, M.; Jezowska-Bojczuk, M.; Kozłowski, H.; Bouhsina, S. *Polyhedron* **1997**, *16*, 3447–3454.

(14) Heineke, D.; Franklin, S. J.; Raymond, K. N. *Inorg. Chem.* **1994**, *33*, 2413–2421.

(15) Eriksson, G. *Anal. Chim. Acta* **1979**, *112*, 375–383.

(16) Smith, R. M.; Martell, A. E. *Critical Stability Constants*; Plenum Press: New York, 1989; Vol. 6.

(17) Baes, C. F.; Mesmer, R. E. *The Hydrolysis of Cations*; John Wiley and Sons: New York, 1976.

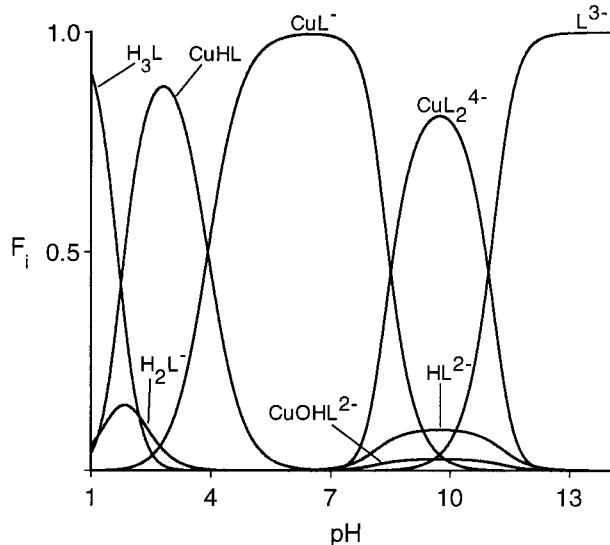
Table 1

(a) Equilibrium Constants from the Literature,<sup>16</sup> Used To Determine the pH and Mixing Ratios That Allow Each Individual Complex To Dominate in Solution

equilib reactn	log $K^a$ (25 °C) $I = 0.1$ M	equilib reactn	log $K^a$ (25 °C) $I = 0.1$ M	equilib reactn	log $K^a$ (25 °C) $I = 0.1$ M
$H^+ + L^{3-} \rightleftharpoons HL^{2-}$	10.14	$Cu^{2+} + L^{3-} \rightleftharpoons CuL^-$	11.93	$CuL^- + H^+ \rightleftharpoons CuHL$	3.92
$H^+ + HL^{2-} \rightleftharpoons H_2L^-$	5.46	$Cu^{2+} + 2L^{3-} \rightleftharpoons CuL_2^{4-}$	16.02	$CuOHL^{2-} + H^+ \rightleftharpoons CuL^-$	9.87
$H^+ + H_2L^- \rightleftharpoons H_3L$	2.20				

(b) Solution Concentrations, pH Values, and Relative Amounts of Dominating Complex in All IR and EXAFS Samples

	IR				EXAFS			
	[L] <sub>tot</sub> (mM)	[Cu] <sub>tot</sub> (mM)	pH (or pD)	% [L] <sub>tot</sub> in complex	[L] <sub>tot</sub> (mM)	[Cu] <sub>tot</sub> (mM)	pH	% [Cu] <sub>tot</sub> in complex
in H <sub>2</sub> O								
L <sup>3-</sup>	24		12.3	~99				
HL <sup>2-</sup>	24		8.2	~99				
H <sub>2</sub> L <sup>-</sup>	24		4.0	~95				
H <sub>3</sub> L	24		1.0	~94				
in D <sub>2</sub> O								
L <sup>3-</sup>	30		13	~100				
DL <sup>2-</sup>	30		8	~99				
D <sub>2</sub> L <sup>-</sup>	30		4	~95				
D <sub>3</sub> L	30		1	~94				
CuL <sup>-</sup>	24	24	6.4	~100	36	30	5.6	~98
CuHL	24	40	2.9	~87	77	23	2.6	~92
CuL <sub>2</sub> <sup>4-</sup>	24	12	9.6	~80	67	25	9.6	~97

<sup>a</sup> The same log  $K$  values were used for the deuterated complexes (DL<sup>2-</sup>, D<sub>2</sub>L<sup>-</sup>, D<sub>3</sub>L) as they are not expected to differ significantly.**Figure 2.** Example of Cu(II)–PMG speciation diagram generated with the program Solgaswater: IR sample of CuHL.  $F_i$  is the fraction of PMG found in respective solution species. [Cu(II)] = 40 mM, [PMG] = 24 mM.

**IR Spectroscopy.** Attenuated total reflectance (ATR) IR spectra were collected using a Perkin-Elmer 2000 FTIR spectrometer fitted with a deuterated triglycine sulfate (DTGS) detector. The spectra were recorded with a horizontal ATR accessory and a diamond crystal as the reflection element (SensIR Technologies). The sample cell was purged with nitrogen gas throughout data collection to exclude carbon dioxide and water vapor. The angle of incidence for the setup is approximately 45°, which is far from the critical angle. This and the fact that the bands analyzed are weak (<0.05 absorbance units), and do not overlap with stronger bands (except for the asymmetric C–O stretch which overlaps with the intense H<sub>2</sub>O bend), indicate that the effects of possible distortions known to occur in ATR spectra are minimized.<sup>18</sup> The solutions were applied to the diamond crystal surface directly, and a

quartz lid was placed over the sample and pressed tightly against a rubber gasket. This sealed the sample from the atmosphere during data collection. One hundred scans were collected for each sample over the range 370–7800 cm<sup>-1</sup>. The sample spectra were interpreted after subtracting spectra of both the empty cell and either 0.1 M NaCl (H<sub>2</sub>O-based solutions) or D<sub>2</sub>O and HDO (D<sub>2</sub>O-based solutions).

**Ab Initio Frequency Calculations.** Theoretical vibration frequencies of deprotonated PMG (L<sup>3-</sup>) and the protonated PMG species (HL<sup>2-</sup>, H<sub>2</sub>L<sup>-</sup>, and H<sub>3</sub>L) were calculated with the Hartree–Fock (HF) restricted method. Four water molecules were included in order to simulate the hydration. In the input structure, these were placed such that the carboxylate group was solvated by one water molecule, and the phosphonate group by three water molecules. The calculations were performed with the program Gaussian 94W, and visualization of the calculated vibrational modes was accomplished with HyperChem v. 5. The standard 3-21G\* basis set was used in all calculations. The potential energy minimum structures of the PMG species were obtained without applying symmetry restrictions; i.e., all bond lengths, angles, and dihedral angles were allowed to vary. The subsequently calculated vibrational frequencies were scaled by the recommended scale factor 0.9085 (HF/3-21G\*) to account for systematic errors.<sup>19</sup> Only positive frequencies were obtained which show that the optimized structures represent a minimum at the potential energy surface.

**EXAFS.** Cu K-edge EXAFS data were measured at the Stanford Synchrotron Radiation Laboratory, California, on beam line 4-1. The ring energy was 3.0 GeV with ring current between 60 and 100 mA. A Si(220) double-crystal monochromator was used and detuned 50% to eliminate higher harmonics. The data were measured at room temperature in the fluorescence mode, with a Lytle detector<sup>20</sup> filled with argon gas. A Ni-6 filter and Soller slit setup were used to reduce K<sub>β</sub> fluorescence and scattering contributions to the signal. Internal calibration was performed by simultaneously measuring spectra from a Cu foil in transmission mode, throughout the duration of all scans. Three to four scans were collected per sample.

Data reduction was performed with EXAFSPAK.<sup>21</sup> Individual scans were calibrated, with the first inflection point of the Cu foil assigned

(18) Urban, M. W. *Attenuated Total Reflectance Spectroscopy of Polymers*; American Chemical Society: Washington, DC, 1996.(19) Foresman, J. B.; Frisch, E. *Exploring Chemistry with Electronic Structure Methods*; Gaussian Inc.: Pittsburgh, 1996.(20) Lytle, F. W.; Greeger, R. B.; Sandstrom, D. R.; Marques, D. R.; Wong, J.; Spiro, C. L.; Huffman, G. P.; Huggins, F. E. *Nucl. Instrum. Methods* **1984**, 226, 542–548.

at 8980.3 eV, and the scans for a particular sample were averaged. A polynomial preedge function and a suitable spline were subtracted from each averaged spectrum, and the data were normalized. Resulting data were analyzed in the  $k$ -region  $3.2\text{--}12.4 \text{ \AA}^{-1}$ ,<sup>22</sup> and the data were fit using the optimization procedure, OPT, in EXFASPAK. Phase and amplitude functions were calculated using FEFF 7.0,<sup>23</sup> with input data based on the X-ray crystal structure of the 1:1 Cu(II) chelate of PMG.<sup>7</sup> Coordination numbers,  $N$ , were kept constant during each optimization although different coordination numbers were tested to find the best fit. During the final fitting procedure, coordination numbers,  $N$ , were fixed, while distance,  $R$ , and Debye–Waller factor,  $\sigma^2$ , were varied. Energy shift,  $\Delta E_0$ , was allowed to vary but kept internally constant for all shells within a particular complex.

## Results and Discussion

### IR Spectroscopy. Speciation of PMG in Aqueous Solution.

A spectrum of the deprotonated PMG molecule ( $L^{3-}$ ) is presented in Figure 3a. The spectrum can be divided into two parts, corresponding to the different donor groups of the ligand. Between 1300 and 1800  $\text{cm}^{-1}$  strong peaks are found, predominantly associated with stretching motions of the carboxylate group, while the region 800–1200  $\text{cm}^{-1}$  is dominated by peaks originating from the phosphonate. This rough assignment is in agreement with the vast literature on IR spectroscopy of carboxylates and phosphonates/phosphates.<sup>24,25</sup> Although discussions in the literature are extensive, the following interpretation provides a summary and serves as a basis for a more detailed interpretation of the zwitterionic nature of PMG and the associated intramolecular hydrogen bonding. The results of our *ab initio* frequency calculations are compared with our experimental data in Table 2. The detailed peak assignment was accomplished by comparing the relative order and the relative intensities of the calculated peaks with the experimental spectra. The assignments are in agreement with previous assignments of carboxylates and phosphonates/phosphates.<sup>24–27</sup> The peaks at 1568 and 1406  $\text{cm}^{-1}$  are assigned to the asymmetric and symmetric  $\text{CO}_2$  stretches ( $\nu_{\text{C-O}^{\text{a}}}$  and  $\nu_{\text{C-O}^{\text{s}}}$ ), respectively. Visualization of the calculated modes indicates that these are relatively pure stretching modes of the carboxylate group. In contrast, the 1319  $\text{cm}^{-1}$  peak is assigned to a complex vibration involving the amine and the methylene groups. The strong peaks at 978 and 1067  $\text{cm}^{-1}$  are assigned to P–O stretching motions of the phosphonate moiety. The former originates from a symmetric P–O stretch, and the latter is predicted to involve three closely spaced and similar asymmetric P–O modes. It is of interest to compare this part of the spectrum with that of hydrogen phosphate ( $(\text{HO})\text{PO}_3^{2-}$ ) since the local symmetry of the P environment can in both cases be described as pseudo- $C_{3v}$ . Accordingly, the P–O modes are very similar, the only difference being that the peaks in hydrogen phosphate are shifted  $\sim 15 \text{ cm}^{-1}$  to higher frequencies.<sup>26,27</sup>

Adding a proton to form  $\text{HL}^{2-}$  induces significant changes in the IR spectrum (Figure 3a). The  $\nu_{\text{C-O}^{\text{a}}}$  is shifted to higher

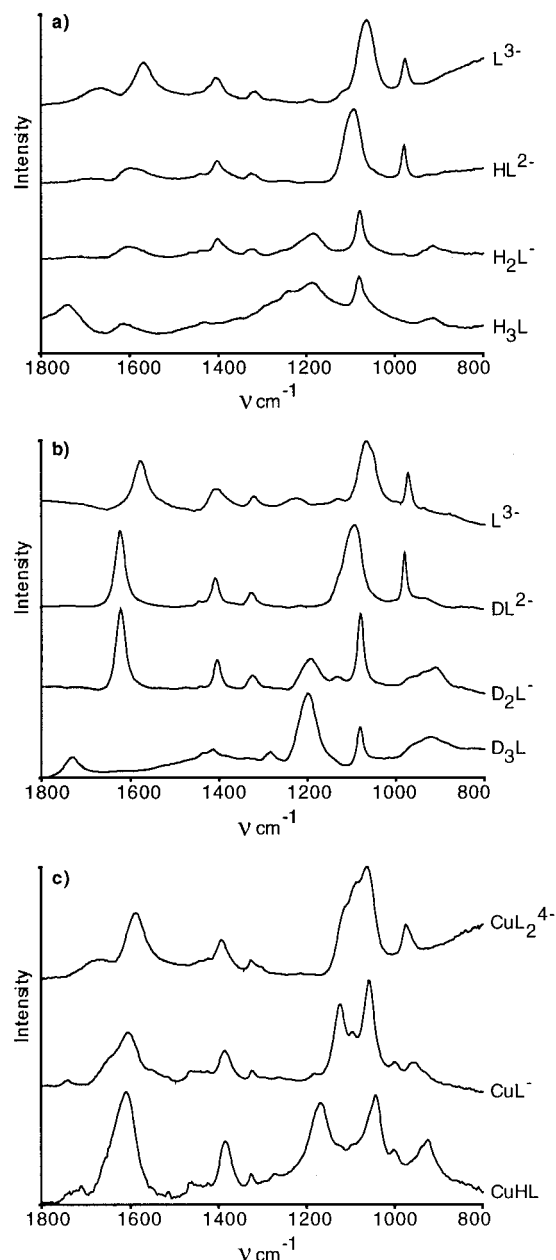


**Figure 3.** FTIR spectra: (a) PMG protonation in  $\text{H}_2\text{O}$ , (b) PMG protonation in  $\text{D}_2\text{O}$ , and (c) Cu(II)–PMG complexes in  $\text{H}_2\text{O}$ .

frequency and broadened. A significant shoulder on the low-frequency side of this peak is also developed; curve-fitting resolves two peaks at 1605 and 1570  $\text{cm}^{-1}$ . These features are indicative of a zwitterionic structure involving  $\text{RCO}_2^-$  and  $\text{R}_2\text{-NH}_2^+$ , where the carboxylate group is hydrogen bonded to the protonated nitrogen atoms.<sup>28</sup> Previous studies have assigned the high-frequency peak to  $\nu_{\text{C-O}^{\text{a}}}$  and the one at lower frequency to a deformation mode of the protonated amine group ( $\delta_{\text{N-H}}$ ). This is in agreement with our experiments in  $\text{D}_2\text{O}$  where the mass effect causes a downward shift of the  $\delta_{\text{N-H}}$  mode, while the  $\nu_{\text{C-O}^{\text{a}}}$  is slightly raised due to decoupling (Figure 3b and Table 2). Accordingly we assign the 1605  $\text{cm}^{-1}$  peak to  $\nu_{\text{C-O}^{\text{a}}}$  and the 1570  $\text{cm}^{-1}$  peak to the  $\delta_{\text{N-H}}$  mode. Formation of the zwitterionic structure is accompanied by a slight shift of  $\nu_{\text{C-O}^{\text{s}}}$  to 1404  $\text{cm}^{-1}$ . The asymmetric P–O stretch experiences an upward shift to 1095  $\text{cm}^{-1}$ , which is indicated by the *ab initio*

(21) George, G. N. *EXAFSPAK*; Stanford Synchrotron Radiation Laboratory: Stanford, 1995.

(22)  $k$  is the photoelectron wave vector;  $k = (2\pi/h)\sqrt{2m(E - E_0)}$  where  $h$  is the Planck constant,  $m$  is electron mass, and  $E_0$  is the energy for the onset of the EXAFS.

(23) Ankudinov, A. L.; Ravel, B.; Rehr, J. J.; Conradson, S. D. *Phys. Rev. B* **1998**, *58*, 7565–7576.

(24) Colthoup, N. B.; Daly, L. H.; Wiberly, S. E. *Introduction to Infrared and Raman Spectroscopy*; Academic Press: New York, 1974.

(25) Nakamoto, K. *Infrared and Raman Spectra of Inorganic and Coordination Compounds*; Wiley: New York, 1986.

(26) Tejedor-Tejedor, M. I.; Anderson, M. A. *Langmuir* **1990**, *6*, 602–611.

(27) Persson, P.; Nilsson, N.; Sjöberg, S. *J. Colloid Interface Sci.* **1996**, *177*, 263–275.

(28) Diem, M. *Introduction to Modern Vibrational Spectroscopy*; Wiley: New York, 1993.

**Table 2.** The Main Experimental and Theoretical IR Frequencies of Aqueous PMG Species ( $\text{cm}^{-1}$ ). Tentative Assignments

assignment	$\text{L}^{3-}$		$\text{HL}^{2-}$		$\text{H}_2\text{L}^-$		$\text{H}_3\text{L}$	
	expt	theor	expt	theor	expt	theor	expt	theor
$\nu_{\text{C}=\text{O}}$							1740 (1733)	1745
$\nu_{\text{C}-\text{O}^{\text{a}}}$	1568 (1581) <sup>a</sup>	1569	1605 (1622)	1648	1610 (1624)	1693		
$\delta_{\text{N}-\text{H}}$			1570 (1133)	1565	1587 (1135)	1585	1617	1581
complex <sup>b</sup>							1431 (1414)	1475
$\nu_{\text{C}-\text{O}^{\text{s}}}$	1406 (1405)	1333	1404 (1406)	1316	1402 (1406)	1270		
complex <sup>b</sup>	1319 (1322)	1306	1325 (1326)	1236	1325 (1326)	1229		
$\nu_{\text{P}-\text{O}^{\text{a}}}$							1295 (1286)	1249
complex <sup>b</sup>							1278	1275
complex <sup>b</sup>							1247	1249
$\nu_{\text{P}-\text{O}^{\text{a}}}$	1190	1230			1248	1270		
$\nu_{\text{P}-\text{O}^{\text{a}}}$	1119 (1135)				1186 (1188)	1184	1185 (1193)	1182
$\nu_{\text{P}-\text{O}^{\text{a}}}$	1067 (1069)	1160, 1130	1095 (1093)	1101, 1068	1081 (1081)	1092	1083 (1083)	1076
$\nu_{\text{P}-\text{O}^{\text{a}}} + \nu_{\text{P}-\text{C}}$							936	969
$\nu_{\text{P}-\text{O}^{\text{s}}}$	978 (974)	954	979 (978)	929	916 (911)	941	914 (919)	940

<sup>a</sup> Values in parentheses are for measurements in  $\text{D}_2\text{O}$ . <sup>b</sup> Mode involving motions of the carbon backbone coupled with C–O and P–O stretching motions.

calculations to be due to hydrogen bonding to  $\text{R}_2\text{NH}_2^+$ . In summary, IR spectroscopy shows  $\text{HL}^{2-}$  to be zwitterionic with the carboxylate and phosphonate groups intramolecularly hydrogen bonded to  $\text{R}_2\text{NH}_2^+$  as depicted in Figure 1.

The spectrum of  $\text{H}_2\text{L}^-$  (Figure 3a) is practically identical to that of  $\text{HL}^{2-}$  in the carboxylate frequency region, but significant differences are detected in the P–O modes. This indicates that the zwitterionic structure, which involves  $\text{RCO}_2^-$  and  $\text{R}_2\text{NH}_2^+$ , is intact and that the second proton binds to a P–O group. The new P–O peaks are very similar to the spectrum of dihydrogen phosphate ( $(\text{OH})_2\text{PO}_2^-$ ), and in analogy with this species and in agreement with the ab initio calculations, we assign the 1186 and 1081  $\text{cm}^{-1}$  peaks to stretching motions of the nonprotonated P–O groups and the 916  $\text{cm}^{-1}$  peak to a P–(OH) stretch.<sup>26,27</sup>

The last protonation step investigated, i.e., the formation of  $\text{H}_3\text{L}$ , is accompanied by significant changes in the carboxylate frequency region. The  $\nu_{\text{C}-\text{O}^{\text{a}}}$  and  $\nu_{\text{C}-\text{O}^{\text{s}}}$  disappear, and new peaks appear at 1740  $\text{cm}^{-1}$  and between 1200 and 1300  $\text{cm}^{-1}$ . These are characteristic for carboxylic acid groups (RCOOH) where the 1740  $\text{cm}^{-1}$  peak is assigned to a C=O stretch and the peaks in the region 1200–1300  $\text{cm}^{-1}$  are coupled C–(OH) stretching and C–O–H bending motions.<sup>29</sup> The P–O peaks discussed above for  $\text{H}_2\text{L}^-$  shift less than 3  $\text{cm}^{-1}$ , which indicates that protonation of the carboxylate group is not accompanied by an intramolecular proton transfer from the nitrogen atom to a P–O group. The interpretation implies that  $\text{H}_3\text{L}$  is still in a zwitterionic form as suggested by Motekaitis and Martell.<sup>9</sup> However, in this structure,  $\text{R}_2\text{NH}_2^+$  mainly hydrogen bonds to the phosphonate end of the molecule. Further support is provided by the peak at 1614  $\text{cm}^{-1}$ , which we tentatively assign to a  $\delta_{\text{N}-\text{H}}$  mode. In agreement with the assignment, this peak is shifted to lower frequency in  $\text{D}_2\text{O}$  (Figure 3b and Table 2). Compared to  $\text{HL}^{2-}$  and  $\text{H}_2\text{L}^-$  the deformation mode in  $\text{H}_3\text{L}$  occurs at a higher frequency. We believe this to be caused by the formation of RCOOH and the concurrent loss of coupling between the  $\nu_{\text{C}-\text{O}^{\text{a}}}$  and the  $\delta_{\text{N}-\text{H}}$  modes.

#### IR Spectra of Cu–PMG Complexes in Aqueous Solution.

The assignments for the  $\text{CuL}^-$  spectrum will be based on the discussion above (the  $\text{L}^{3-}$ ,  $\text{HL}^{2-}$ ,  $\text{H}_2\text{L}^-$ , and  $\text{H}_3\text{L}$  assignments) and literature data. No ab initio frequency calculations were attempted. The carboxylate frequency region displays two strong peaks at 1606 and 1387  $\text{cm}^{-1}$  (Figure 3c), which are assigned to  $\nu_{\text{C}-\text{O}^{\text{a}}}$  and  $\nu_{\text{C}-\text{O}^{\text{s}}}$ , respectively. The  $\nu_{\text{C}-\text{O}^{\text{a}}}$  peak has a shoulder

**Table 3.** The Main Experimental IR Frequencies of Aqueous Cu(II)–PMG Complexes ( $\text{cm}^{-1}$ ). Tentative Assignments

assignment	$\text{CuL}^-$	$\text{CuHL}$	$\text{CuL}_2^{4-}$
$\nu_{\text{C}-\text{O}^{\text{a}}}$	1606	1610	1588
$\nu_{\text{C}-\text{O}^{\text{s}}}$	1387	1385	1394
	1323	1325	1326
$\nu_{\text{P}-\text{O}^{\text{a}}}$	1125	1169	1127
$\nu_{\text{P}-\text{O}^{\text{a}}}$	1096		1101
$\nu_{\text{P}-\text{O}^{\text{a}}}$	1059	1043	1063
$\nu_{\text{P}-\text{O}^{\text{a}}}$	1010	1007	
$\nu_{\text{P}-\text{O}^{\text{s}}}$	957	925	975

at 1625  $\text{cm}^{-1}$  that is tentatively assigned to the bending mode of the water molecules in the first coordination sphere. Separation of the  $\nu_{\text{C}-\text{O}^{\text{a}}}$  and  $\nu_{\text{C}-\text{O}^{\text{s}}}$ ,  $\Delta$ , of  $\text{CuL}^-$  is increased 56  $\text{cm}^{-1}$  in comparison with  $\text{L}^{3-}$ . For acetate, such shifts have been shown to be indicative of a monodentate coordination to metal ions.<sup>30</sup> Accordingly, the IR spectrum of  $\text{CuL}^-$  suggests a monodentate linkage between the carboxylate group and Cu(II), which fits the previously proposed structure,<sup>8–11</sup> and the EXAFS scattering paths involving the carboxylate group, which are discussed in the following section. A comparison of the  $\text{L}^{3-}$  and  $\text{CuL}^-$  IR spectra (Figure 3, panels a and c, respectively) reveals strong perturbations of the P–O peaks upon coordination to Cu(II), which in turn implies a direct bond between Cu(II) and the phosphonate group. Again this is in excellent agreement with previous structural descriptions and with the EXAFS data. A more detailed, although tentative assignment of the  $\text{CuL}^-$  IR spectrum is summarized in Table 3.

As for  $\text{CuHL}$ , the IR spectrum clearly indicates protonation of the phosphonate group. The frequencies and intensities of the P–O peaks are markedly different from those of  $\text{CuL}^-$  (Figure 3c and Table 3). Furthermore, the carboxylate peaks are practically unchanged and the spectrum does not contain the  $\delta_{\text{N}-\text{H}}$  peak, which rules out protonation of the amine or the carboxylate group. Both the phosphonate oxygens that are available for coordination to Cu and to H are thus occupied, and in that way  $\text{CuHL}$  resembles  $\text{H}_2\text{L}^-$ . In fact the IR spectra of these species show many similarities in the phosphonate frequency region (Figure 3a,c), and this is used in the peak assignment (Tables 2 and 3).

Considering evidence in the literature concerning bis(glyphosate)metal(III) complexes,<sup>14</sup> it is suspected that the  $\text{CuL}_2^{4-}$  solution contains an isomeric mixture of a relatively large number of species, which makes the IR spectrum of  $\text{CuL}_2^{4-}$

(29) Nordin, J.; Persson, P.; Laiti, E.; Sjöberg, S. *Langmuir* **1997**, *13*, 4085–4093.

(30) Deacon, G. B.; Phillips, R. J. *Coord. Chem. Rev.* **1980**, *33*, 27–250.

Table 4. EXAFSPAK Fit Results<sup>a</sup>

	Cu–N <sub>eq</sub> /O <sub>eq</sub> (SS)			Cu–C (SS)			Cu–P (SS)			Cu–O <sub>d</sub> (SS)			Cu–O–C (MS)			$\Delta E_0$	error <sup>c</sup>
	<i>N</i>	<i>R</i> (Å) ±0.01 <sup>b</sup>	$\sigma^2$	<i>N</i>	<i>R</i> (Å) ±0.03	$\sigma^2$	<i>N</i>	<i>R</i> (Å) ±0.04	$\sigma^2$	<i>N</i>	<i>R</i> (Å) ±0.04	$\sigma^2$	<i>N</i>	<i>R</i> (Å) ±0.04	$\sigma^2$		
CuHL	4	1.96	0.004	3	2.81	0.007	1	3.00	0.006	2	3.72	0.007	2	4.08	0.005	–5.36	0.139
CuL <sup>–</sup>	4	1.96	0.004	3	2.81	0.004	1	3.01	0.006	2	3.72	0.005	2	4.08	0.005	–2.76	0.120
CuL <sub>2</sub> <sup>4–</sup>	4	1.97	0.005	3	2.81	0.003	1	3.06	0.006	2	3.73	0.006	2	4.11	0.008	–4.98	0.157
	4	1.98	0.005	5	2.83	0.007	1	3.07	0.010	2	3.74	0.006	2	4.12	0.007	–4.07	0.141
	3.5	1.97	0.004	3	2.81	0.003	1	3.06	0.006	2	3.73	0.007	2	4.11	0.007	–4.45	0.150
	<b>3.5<sup>d</sup></b>	<b>1.98</b>	<b>0.004</b>	<b>5</b>	<b>2.83</b>	<b>0.007</b>	<b>1</b>	<b>3.08</b>	<b>0.010</b>	<b>2</b>	<b>3.74</b>	<b>0.006</b>	<b>2</b>	<b>4.13</b>	<b>0.007</b>	<b>–3.64</b>	<b>0.131</b>

<sup>a</sup> For final fits: coordination number (*N*), fixed, distance (*R*) and Debye–Waller factor ( $\sigma^2$ ) varied. Energy shifts,  $\Delta E_0$ , were allowed to vary but kept internally constant for all shells within a complex. The amplitude reduction factor *S*<sub>0</sub> was kept constant at a value of 0.9, determined from the reference compound Cu(OH)<sub>2</sub>. N<sub>eq</sub>/O<sub>eq</sub> represents equatorial atoms in the first coordination sphere. O<sub>d</sub> represents a distal oxygen atom (i.e., not bonded to the absorbing copper atom). <sup>b</sup> Error estimated from least-squares fitting, values are valid for 95% confidence limits. <sup>c</sup> Fit error, defined as  $\sum k^6(\chi_{\text{exptl}} - \chi_{\text{calcd}})^2 / \sum k^6 \chi_{\text{exptl}}^2$ . <sup>d</sup> Values in bold type show the fit resulting in the lowest fit error.

difficult to interpret and assign. The overall features are similar to the CuL<sup>–</sup> spectrum (Figure 3c and Table 3). The  $\nu_{\text{C–O}^{\text{a}}}$  and  $\nu_{\text{C–O}^{\text{s}}}$  are slightly shifted, and  $\Delta$  is decreased. This could suggest that, on average, the carboxylate groups are less strongly coordinated to Cu(II), in agreement with an axial position of some of these groups. The shoulder at 1625 cm<sup>–1</sup> is missing in the spectrum, which supports our assignment, since no water molecules are expected in the first coordination sphere of CuL<sub>2</sub><sup>4–</sup>. P–O peaks are detected at frequencies similar to those of CuL<sup>–</sup>. However, the relative intensities are different and the peak resolution is much worse. This is ascribed to the fact that coordinated PMG is present in a range of chemical states (i.e., in both equatorial and axial positions) caused by the existence of several CuL<sub>2</sub><sup>4–</sup> isomers.

**EXAFS.** The results from the EXAFS fitting procedure are summarized in Table 4. In each case, the goodness of fit was assessed with the fit error (see footnote, Table 4). For all three complexes, the data were best fit with four single scattering (SS) paths and a multiple scattering (MS) path. Attempts to include copper as a backscatterer did not result in good fits, and the possibilities of polymerization or colloidal precipitation of a copper-containing solid phase were therefore ruled out.

All three EXAFS spectra are strikingly similar (Figure 4), and the Fourier transform (FT) of the data shows three shells at different distances, *R* (uncorrected for phase shift), away from the absorbing copper atom. The biggest difference is a marked decrease in magnitude of the Fourier transformed signal for the first shell of the CuL<sub>2</sub><sup>4–</sup> complex.

The CuL<sup>–</sup> complex has been discussed more extensively than CuHL and CuL<sub>2</sub><sup>4–</sup> in the literature and thus provides a good starting point for discussion. The first shell was best fit with four oxygen/nitrogen atoms at an average distance of 1.96 Å from the absorbing copper atom. These four atoms are most likely positioned in the equatorial plane of a Jahn–Teller distorted, elongated octahedron, similar to the arrangement described for Cu(OH)<sub>2</sub>.<sup>31</sup> The more distant axial oxygens of the octahedron form weaker bonds with the copper atom, giving rise to higher thermal disorder. These atoms are therefore not expected to contribute significantly to the EXAFS signal. Attempts to fit oxygen at axial positions indeed resulted in high Debye–Waller factors for these atoms (>0.02), and there was no significant improvement in the fit, compared to including only equatorial oxygen/nitrogen atoms.

The second shell of neighboring atoms was best fit with three carbon atoms at an average distance of 2.81 Å, and one phosphorus atom at a distance of 3.01 Å. Taking these values

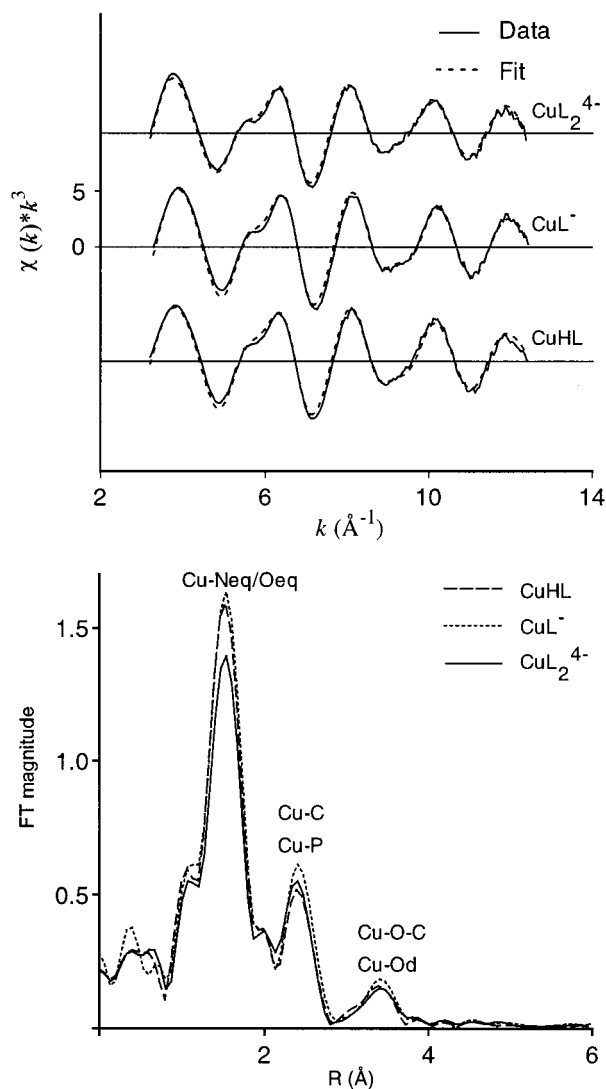
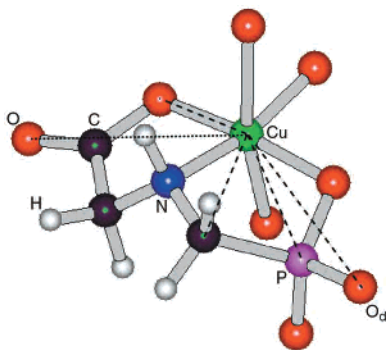


Figure 4. *k*<sup>3</sup>-weighted EXAFS spectra (data and fit) and respective Fourier transforms of the data (not corrected for phase shift) for the Cu(II)–PMG complexes.

into account, the most likely structural interpretation is that two chelate rings and a water of hydration are located in the equatorial plane with all three donor ligands involved in chelating and the remaining water of hydration of the first coordination sphere occupying axial positions. The structure is represented in Figure 5 and agrees well with the findings of Daniele et al.<sup>8</sup> and Glass.<sup>11</sup> The results verify that the five-membered chelate rings identified in the X-ray crystal structure



**Figure 5.** Molecular structure of  $\text{CuL}^-$  (not to scale). The dashed lines represent the four single scattering paths, and the dotted line represents the multiple scattering path, identified in the EXAFS data analysis and described in the text.  $\text{O}_d$  represents a distal oxygen atom (i.e., not bonded to the absorbing copper atom).

of the  $\text{Cu(II)}$  chelate of  $\text{PMG}^7$  are also intact when  $\text{Cu}$  and  $\text{PMG}$  form  $\text{CuL}^-$  in solution.

Fitting the EXAFS data for the protonated complex,  $\text{CuHL}$ , resulted in the same distances and coordination numbers as for  $\text{CuL}^-$ , with only a slight increase in the Debye–Waller factors of the second-shell features and the distal oxygens. This clearly shows that the structure of  $\text{CuHL}$  is essentially identical to that proposed for  $\text{CuL}^-$ , i.e., two chelate rings and a water molecule occupying an equatorial plane.

It is not possible to define a single structure for the 1:2 complex from the EXAFS data, and as expressed earlier, it is believed that the 1:2 complex does indeed form a mixture of isomers in solution. The distances and coordination numbers given therefore represent a weighted average of all the existing isomers, with more dominant isomers providing a greater contribution to the EXAFS signal. Although EXAFS data analysis using the same coordination numbers as in the 1:1 complexes and distances similar to those of the 1:1 complexes provided a reasonable fit, a significant improvement in the fit was obtained by systematically varying the coordination numbers in both the first and second shells (see different fit results listed in Table 4). A decrease in magnitude compared to the 1:1 complexes is found in the first transition of the FT (Figure 4). This is to be expected for a mixture of isomers. Different arrangements of the donor ligands around the central  $\text{Cu}$  atom would cause slight differences in the  $\text{Cu}-\text{O}$  bond lengths, depending on the geometry of the complex, i.e., whether the ligands are equatorially bound, axially bound, or a combination of both. These slightly out of phase contributions to the overall signal would to some extent cancel each other out, leading to a decrease in magnitude of the signal and an apparent decrease in coordination number. The best fit for the first shell gave a coordination number of 3.5. Increasing the number of carbon backscatters in the second shell also produced a better fit to the data. This is conceivably due to the presence of two ligands coordinated in some way to the absorbing copper atom. Note that the coordination number of 1 for phosphorus (Table 4) in this 1:2 complex is the same value as for the 1:1 complex. This implies that if two phosphonate donors are bound to the copper, one is bound at an equatorial position, with low enough thermal disorder to contribute significantly to the EXAFS signal, while the other is bound at an axial position, forming a weaker bond. This axial phosphonate group experiences relatively more disorder, enough that it does not seemingly contribute to the EXAFS signal. There are therefore indications that more dominant isomers have  $\text{PMG}$  ligands bound to copper(II), via

equatorial and axial positions, with both phosphonate and carboxylate donor groups responsible for chelation at the axial positions.

The slight tendency of the bond distances,  $R$ , to increase in the 1:2 complex compared with the 1:1 complexes, for all the paths identified, is likely to be the steric effect of an increased number of neighbors accommodated around the central copper ion.

The existence of chelate rings in the equatorial plane of the structures is strongly supported by the third shell observed in the FT of the data (Figure 4), which is interpreted in a similar manner for all three complexes. The distal oxygen atoms (those not coordinated to the copper atom) of the phosphonate group and the carboxylate group provided a good fit to the data by including both contributions from single scattering paths,  $\text{Cu}-\text{O}_d$  (Figure 5), and that of a multiple scattering path through the carbon atom (Figure 5). According to the FEFF calculations, these particular paths were predicted to have relatively large amplitude ratios (44% and 40%, respectively, for a coordination number of 2, while the amplitude ratio of a first-shell oxygen is predicted to be 90–100%). The contributions can be justified by the rigidity of the structure provided by the chelate ring, together with a  $\text{Cu}-\text{C}-\text{O}$  bond angle that is sufficiently linear for multiple scattering effects to become significant. Fitts et al.<sup>32</sup> describe similar contributions from a third shell in glutamate–copper(II) complexes. The single scattering path was best fit with a coordination number of 2, and this is believed to represent the distal oxygens of the phosphonate group. Although the distal oxygen of the carboxylate could provide an alternative explanation, the average distance of 3.71–3.73 Å obtained in the final fit does not agree well with the 4.06–4.11 Å multiple scattering distance of this oxygen.

## Summary

Different steps of  $\text{PMG}$  protonation have been identified and structures of  $\text{Cu(II)}-\text{PMG}$  complexes in aqueous solution have been characterized with IR and EXAFS spectroscopic measurements and ab initio frequency calculations. The IR results and ab initio calculations indicate that protonation of  $\text{L}^{3-}$  forms a  $\text{HL}^{2-}$  zwitterion whereby the carboxylate and phosphonate donor groups are intramolecularly hydrogen-bonded to the amine group,  $\text{R}_2\text{NH}_2^+$ . The zwitterion remains intact on progressing to  $\text{H}_2\text{L}^-$ , and the second proton resides on the phosphonate group. For  $\text{H}_3\text{L}$ , the structure is still zwitterionic but intramolecular hydrogen bonding is predominantly between the phosphonate and amine groups only and a  $\text{COOH}$  group is formed.

Structures of  $\text{CuL}^-$ ,  $\text{CuHL}$ , and  $\text{CuL}_2^{4-}$  contain five-membered chelate rings with the amine, carboxylate, and phosphonate groups of the  $\text{PMG}$  ligand all involved in chelation. For  $\text{CuL}^-$ , evidence of monodentate linkage to carboxylate and a direct bond to the phosphonate were identified with IR and there was evidence for  $\text{H}_2\text{O}$  molecules in the first coordination sphere. The EXAFS data confirmed these findings, indicating two chelate rings oriented in the equatorial plane, with all three donor groups of the  $\text{PMG}$  molecule responsible for chelation.  $\text{CuHL}$  was found to be essentially identical to  $\text{CuL}^-$ , differing only in the protonation of the phosphonate group, as identified by IR. Although a single definitive structure of the  $\text{CuL}_2^{4-}$  complex could not be identified, there is substantial evidence for the existence of several isomers. IR spectral features for  $\text{CuL}_2^{4-}$  are similar to those for  $\text{CuL}^-$ , but peaks in the

(32) Fitts, J. P.; Persson, P.; Brown, G. E., Jr.; Parks, G. A. *J. Colloid Interface Sci.* **1999**, *220*, 133–147.

carboxylate region suggest that at least some carboxylate groups must be chelated at axial positions. The absence of a peak representing H<sub>2</sub>O molecules in the first coordination sphere indicates the chelation of PMG donors at both equatorial and axial positions while the phosphonate peaks suggest the coordinated PMG to be present in a range of chemical states. EXAFS results also point toward an isomeric mixture of complexes, primarily indicated by a loss in magnitude in the first transition of the Fourier transformed EXAFS data.

These results form the basis for forthcoming studies of ternary surface complexes formed from adsorption of Cu(II) and PMG onto mineral oxide surfaces.

**Acknowledgment.** This work was supported by the Swedish Natural Science Research Council. We thank the staff of Stanford Synchrotron Radiation Laboratory (SSRL), particularly

Dr. John Bargar, for their help and advice. SSRL is operated by the Department of Energy, Office of Basic Energy Sciences. We also acknowledge the National Institutes of Health, National Center for Research Resources, Biomedical Technology Program, and the Department of Energy Office of Biological and Environmental Research (OBER), which support the SSRL Structural Molecular Biology Program, whose instrumentation was used for the measurements. The Kempe Foundation, Sweden, and the OBER are acknowledged for providing financial support for the educational stay of Julia Sheals at SSRL. Professor Staffan Sjöberg is acknowledged for his valuable comments on the manuscript and Dr. Magnus Karlsson for his assistance with the illustrations. Mrs. Agneta Nordin is gratefully acknowledged for help with the IR measurements.

IC000849G